Supplementary Information

Vacancy-Mediated Enhancement of Interfacial Thermal Transport in Si/SiC Heterojunctions: A Molecular Dynamics Study

S1 Structural Integrity Analysis via Radial Distribution Function (RDF)

To verify that the introduction of high concentrations of vacancies (up to 30%) does not induce substantial structural disordering or amorphization in the SiC lattice, we computed the radial distribution function, $g(r)$, for both the defective and pristine configurations. This analysis addresses concerns regarding whether the observed thermal transport behavior might be an artifact of amorphization.

Figure S1 compares the partial RDFs of the system with 30% vacancies (Fig. S1a) against those of the pristine, defect-free system (Fig. S1b). The RDFs are decomposed into contributions from C–C, C–Si, and Si–Si pairs. In both cases, the RDFs exhibit a sequence of sharp coordination peaks with well-defined positions. Crucially, these peaks remain discernible at larger radial distances ($r > 5$ Å), indicating that the interatomic distance distribution retains strong discreteness and repeatability. This behavior is the hallmark of long-range crystalline order.

In contrast, amorphization or local melting would typically lead to a pronounced broadening of the first coordination peak and a rapid smearing-out of subsequent peaks into a smooth, featureless background at larger distances. A direct comparison between Fig. S1(a) and (b) shows that the major peak positions and sequences are essentially unchanged. The observed differences are limited to reduced peak intensities and slight broadening, which are expected consequences of local coordination loss and atomic relaxation around point defects. Therefore, the RDF analysis confirms that the vacancy-containing system remains a highly defective crystal rather than undergoing a phase transition to an amorphous state.

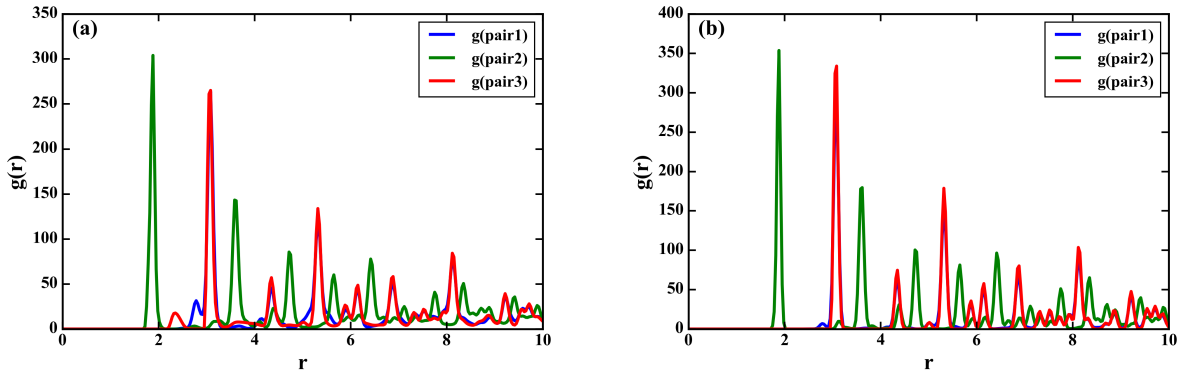

(a) High-Vacancy Case (30%) (b) Pristine Reference

Figure S1: Z-slice–resolved partial radial distribution functions (RDFs) of SiC for (a) the high-vacancy case and (b) the pristine reference. The three curves correspond to C–C, C–Si, and Si–Si pairs. The persistence of sharp peaks at the same neighbor-shell positions in (a) demonstrates that the SiC lattice remains crystalline despite the introduction of vacancies.

S2 Frequency-Resolved Transport: Spectral Decomposition of ITC

To provide direct evidence for the opening of new transport channels via inelastic scattering, we performed a spectral decomposition of the interfacial thermal conductance. Figure S2 presents a comprehensive frequency-resolved analysis comparing the pristine (sharp) interface and the interface with 30% carbon vacancies.

The transmission spectrum (Left Panel) reveals a stark contrast between the two systems. The pristine interface (orange line) is strictly limited to transmission below ∼17 THz, which corresponds to the intrinsic cut-off frequency of the silicon lattice. Conversely, the defected interface (green line) exhibits significant new transmission peaks in the 20–40 THz range. This phenomenon indicates that high-frequency phonons in SiC, which are typically trapped due to the mismatch, are effectively being down-converted to lower frequencies or are coupling inelastically across the interface.

This observation is further corroborated by the spectral conductance $G(\omega)$ (Middle Panel). While the low-frequency contribution (< 15 THz) remains comparable for both cases, the defected interface (blue line) demonstrates substantial conductance contributions in the 20–40 THz band, which are virtually absent in the pristine case. The cumulative integral (Right Panel) confirms that this additional high-frequency contribution acts as the primary driver for the overall enhancement of ITC, raising the total conductance from ∼0.8 GW m^{-2} K^{-1} to over 1.1 GW m^{-2} K^{-1}. Collectively, this analysis provides direct quantitative evidence that the near-interface vacancy layer facilitates inelastic phonon bridging, converting high-frequency SiC modes into transmissible energy carriers.

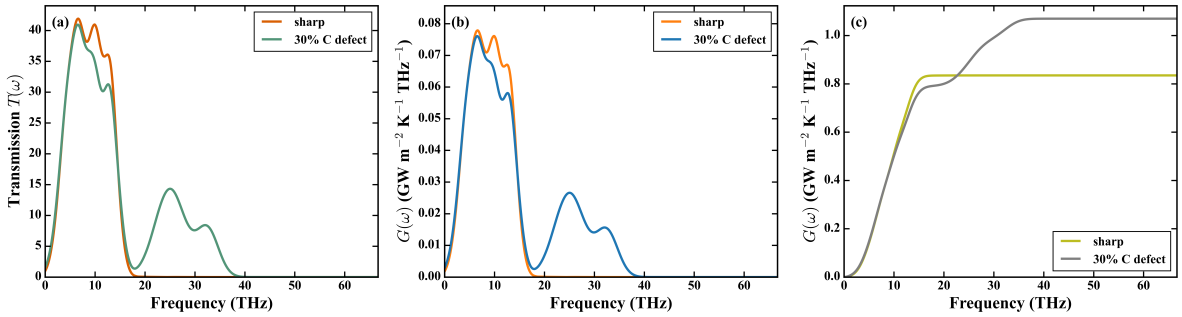

Figure S2: Frequency-resolved thermal transport analysis comparing the pristine (sharp) Si/SiC interface and the interface with 30% C vacancies. **(Left)** Phonon transmission coefficient $T(\omega)$; **(Middle)** Spectral interfacial thermal conductance $G(\omega)$; **(Right)** Cumulative interfacial thermal conductance. The emergence of significant transmission and conductance contributions in the 20–40 THz range for the defected system provides direct evidence of inelastic phonon bridging.

S3 Universality Check: Si(111)/SiC(0001) Interface

To assess the generality of the proposed vacancy-mediated enhancement mechanism and its sensitivity to interface orientation, we performed additional NEMD simulations on a different interface configuration: Si(111)/SiC(0001). This model complements the Si(100)/SiC(0001) configuration presented in the main text. Consistent with the optimal configuration identified for the Si(100) interface, the defect layer was placed at a distance of $d = 10$ Å from the interface.

Figure S3 displays the Interfacial Thermal Conductance (ITC) as a function of vacancy concentration for both Carbon and Silicon vacancies. Introducing 1% vacancies immediately boosts the ITC from the pristine baseline ($\sim$720 MW m^{-2} K^{-1}). Further increasing the concentration leads to a monotonic increase, reaching nearly 900 MW m^{-2} K^{-1} at 5% concentration for both vacancy types. Although the absolute values of ITC differ slightly from the Si(100) case due to differences in interfacial bonding density and atomic stacking, the qualitative trend—a significant enhancement of ITC upon introducing near-interface vacancies—is identical. This result confirms that the enhancement mechanism, driven by the inelastic down-conversion of high-frequency phonons to bridge the spectral mismatch, is robust and largely independent of the specific crystallographic orientation of the interface.

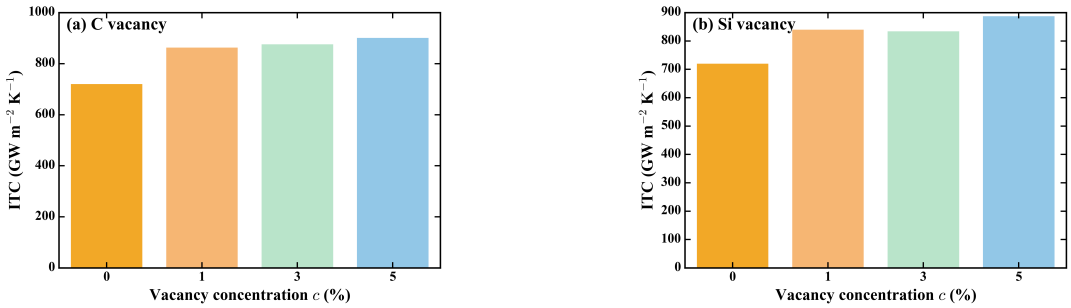

(a) C Vacancy (b) Si Vacancy

Figure S3: Interfacial Thermal Conductance (ITC) of the Si(111)/SiC(0001) interface as a function of vacancy concentration, with the defect layer located at $d = 10$ Å. The pristine interface ($c = 0$) serves as the baseline. Both (a) Carbon and (b) Silicon vacancies induce a significant enhancement in ITC, demonstrating the universality of the mechanism across different crystal orientations.